This article has been accepted for publication in a future issue of this journal, but has not been fully edited. Content may change prior to final publication. Citation information: DOI 10.1109/TII.2022.3180080, IEEE Transactions on Industrial Informatics

Optimal Chiller Loading Based on Collaborative Neurodynamic Optimization

Zhongying Chen, Jun Wang, *Life Fellow, IEEE,* and Qing-Long Han, *Fellow, IEEE*

***Abstract*—Chillers are indispensable machines for heat removal and major sources of power consumption in heating, ventilation, and air conditioning systems. In this paper, a cardinality-constrained global optimization problem is formulated to minimize power consumption for optimal chiller loading. The formulated problem is solved using a collaborative neurodynamic optimization method based on multiple neurodynamic models. Experimental results based on available actual chiller parameters are elaborated to demonstrate the superiority of the proposed approach to many baseline methods for optimal chiller loading.**

***Index Terms*—Optimal chiller loading, neurodynamic optimization, global optimization, HVAC systems, cardinality constraint**

I. Introduction

Heating, ventilation, and air conditioning (HVAC) systems are vital facilities for regulating temperature and humidity in the ambient environments of residential, industrial, and commercial buildings to meet specified thermal comfort and air quality requirements [1]. HVAC systems consume a substantial amount (up to 40%) of energy in commercial buildings [2], [3]. In the global urbanization process, it is anticipated that HVAC systems will take up an increasing portion of energy consumption. In view of the high demands for reducing energy consumption and carbon emission, it is economically beneficial to develop energy-efficient HVAC systems [2], [4].

As essential components of HVAC systems, chillers are thermodynamic devices for removing heat from spaces via coolant circulation. Chillers are responsible for more than 60% of energy consumption in HVAC systems [5]. Optimization plays a crucial role in improving energy efficiency and avoiding excessive energy consumption in chiller systems [6], [7]. Optimal chiller loading (OCL) is a common way to optimize demanded load dispatching among various chillers with minimized power consumption [8].

OCL is tackled by using mathematical programming methods (e.g., [9]–[11]) and meta-heuristic methods (e.g., [10], [12]–[16]). Existing mathematical programming methods include Lagrangian method (LGM) [9], [10], branch and bound (BB) method [11], and cutting-plane (CP) method [11]. Existing heuristic and meta-heuristic methods include genetic algorithm (GA) [10], [12], particle swarm optimization (PSO) algorithm [12], [13], differential evolution (DE) algorithm [14], improved firefly algorithm (IFA) [15], differential cuckoo search approach (DCSA) [16], memetic algorithm [17], heuristic algorithms via dynamic programming and mixed-integer linear programming [18], and neurodynamic optimization [19]–[24], just to name a few.

In some OCL schemes [9], [10], [12], all chillers are assumed to be turned on to meet cooling-load demands. In many scenarios with low demands, it is usually unnecessary to switch on all chillers in service. To save maintenance costs, it is desirable to switch off some chillers [13]–[16]. To address the issue of maintenance costs, OCL is formulated as a mixed-integer nonlinear optimization problem with binary variables for indicating the on/off status of chillers and continuous variables for partial load ratio [11]. The formulation deals with the issue in a complicated way, with binary variables in its objective function as well as a constraint. The formulated problem is solved by using the General Algebraic Modeling System (GAMS) that is a commercial software package consisting of many optimization solvers. The exact methods in GAMS include BB and CP methods that are not time-efficient for solving mixed-integer optimization problems with nonconvex objective functions [25], [26]. The other exact method for OCL (LGM) [9], [10] works for convex optimization only [5].

Since the 1980s, neurodynamic optimization has emerged as a parallel distributed approach to optimization based on recurrent neural networks [19]. Many neurodynamic optimization models have been developed to solve various optimization problems, e.g., [19]–[21]. In recent years, collaborative neurodynamic optimization (CNO) has been developed as a hybrid intelligence framework [22]–[24]. With multiple neurodynamic models for scattered searches and a meta-heuristic rule for neuronal state reinitialization, CNO is proven to be almost surely convergent to global optimal solutions to global and combinatorial optimization problems [22], [23].

In view of the above discussions, this paper addresses cardinality-constrained OCL in HVAC systems. It is formulated as a global optimization problem subject to cardinality, supply-demand, and capacity constraints. A CNO-based OCL method, called CNO-CL, is developed for solving the formulated problem.

The contributions of this paper are highlighted as follows:

1) OCL is formulated as a mixed-integer optimization problem with a cardinality constraint to restrict the number of active chillers. It is further reformulated as a global

This work was supported in part by the Research Grants Council of the Hong Kong Special Administrative Region of China under Grant 11203721 and in part by the Australian Research Council under Grant DP200100700.
(*Corresponding author: Jun Wang.*)

Zhongying Chen and Jun Wang are with the Department of Computer Science, City University of Hong Kong, Hong Kong. Jun Wang is also with the School of Data Science, City University of Hong Kong, Hong Kong (e-mail: zy.chen@my.cityu.edu.hk, jwang.cs@cityu.edu.hk).

Qing-Long Han is with the School of Software and Electrical Engineering, Swinburne University of Technology, Melbourne, VIC 3122, Australia (e-mail: qhan@swin.edu.au).

optimization problem with nonlinear equality constraints and a possibly nonconvex objective function. It enables one to minimize power consumption with optimal partial loading ratios while keeping some chillers off and meeting loading demands in chiller systems.

2) A CNO-based OCL method is customized for solving the reformulated problem with almost sure convergence. It is experimentally demonstrated, based on real chiller data, to be superior to several prevailing OCL methods in terms of solution optimality and variability.

The remaining part of this paper is organized as follows. In Section II, some necessary background knowledge of projection neural networks (PNNs), PSO, and CNO are introduced. In Section III, the OCL problem formulation is described. In Section IV, the CNO-CL algorithm is delineated. In Section V, the experimental results based on four chiller systems are elaborated. Finally, in Section VI, the conclusions are given.

II. Backgrounds

This section provides some background knowledge about PNNs, PSO, and CNO to facilitate the understanding of the proposed methods and experimental results.

A. Projection Neural Networks

Consider a general optimization problem as follows:

$$\begin{aligned} &\min\ f(x) \\ &\text{subject to } g(x) \leq 0,\ h(x) = 0,\ \underline{x} \leq x \leq \overline{x}, \end{aligned} \tag{1}$$

where $x \in \mathbb{R}^n$ is a decision variable, $f(x)$: $\mathbb{R}^n \rightarrow \mathbb{R}$ is an objective function, $g(x) \in \mathbb{R}^p$ and $h(x) \in \mathbb{R}^q$ are respectively the vector-valued functions for inequality and equality constraints, and $\underline{x} \in \mathbb{R}^n$ and $\overline{x} \in \mathbb{R}^n$ are respectively lower and upper bounds of x.

Based on piecewise-linear activation functions (projection operations), a projection neural network (PNN) proposed in [20] for solving box-constrained optimization problems is described as follows:

$$\epsilon \frac{dx}{dt} = -x + P_\Omega(x - \nabla f(x)), \tag{2}$$

where ϵ is a positive constant, $\Omega = \{x \in \mathbb{R}^n \mid \underline{x} \leq x \leq \overline{x}\}$, $\nabla f(x)$ is the gradient of $f(x)$, and

$$P_\Omega(x) = \min\{\max\{\underline{x}, x\}, \bar{x}\} = \begin{cases} \bar{x}, & x > \bar{x}, \\ x, & \underline{x} \leq x \leq \bar{x}, \\ \underline{x}, & x < \underline{x}. \end{cases} \tag{3}$$

In particular, if Ω is the nonnegative quadrant (i.e., $\bar{x} \rightarrow +\infty$ and $\underline{x} = 0$), then a special case of $P_\Omega(x)$ is the popular rectified linear unit (ReLU) defined as $(x)^+ = \max\{0, x\}$.

It is proven in [20] that the PNN is globally convergent to the optimum of constrained convex optimization problems. Furthermore, it is also proven in [21] that the PNN is globally convergent to the optimal solution to pseudoconvex optimization problems.

For global optimization problems with nonconvex functions, a three-layer PNN is proposed in [23] as follows:

$$\begin{cases} \epsilon \frac{dx}{dt} = -x + P_\Omega(x - (\nabla f(x) + \nabla g(x)\lambda + \nabla h(x)v \\ \qquad\qquad + \alpha \nabla g(x) D(\lambda) g(x) + \beta \nabla h(x) h(x))), \\ \epsilon \frac{d\lambda}{dt} = -\lambda + (\lambda + g(x))^+, \\ \epsilon \frac{d\nu}{dt} = h(x), \end{cases} \tag{4}$$

where λ and ν are Lagrange multipliers, α and β are two nonnegative parameters, $\nabla g(x)$ and $\nabla h(x)$ are respectively the gradients of $g(x)$ and $f(x)$, and $D(\lambda)$ is the diagonal matrix of λ. It is proved in [23] that the PNN is globally stable and convergent to a strict local minimum of global optimization problems.

B. Collaborative Neurodynamic Optimization

In the presence of nonconvexity in global optimization, neurodynamic optimization with a single neurodynamic model is vulnerable to being trapped in local minima. In a multimodel framework called collaborative neurodynamic optimization (CNO), multiple neurodynamic models are employed for scatter search of optima and use a meta-heuristic rule for repositioning their neuronal states upon their local convergence to escape from local minima toward global optima.

PNNs are used in most existing CNO paradigms [27], [28]. Other neurodynamic optimization models are also used; e.g., [29]. The PSO rule [30] defined below is used as the meta-heuristic rule in CNO [22], [23], [27]–[29]:

$$\begin{aligned} v_i(\ell+1) =& c_0 v_i(\ell) + c_1 r_1 \left(\tilde{x}_i(\ell) - x_i(\ell)\right) \\ &+ c_2 r_2 \left(\hat{x}(\ell) - x_i(\ell)\right), \\ x_i(\ell+1) =& x_i(\ell) + v_i(\ell+1), \end{aligned} \tag{5}$$

where $x_i(\ell)$ and $x_i(\ell+1)$ are the positions of the ith agent respectively up to the ℓth and $(\ell+1)$th iterations, $v_i(\ell)$ and $v_i(\ell+1)$ are the velocities of the ith agent respectively up to the ℓth and $(\ell+1)$th iteration, c_0 is the inertia weight, c_1 and c_2 are weighting parameters, r_1 and r_2 are two random values in [0,1], $\tilde{x}_i(\ell)$ is the best position recorded by the ith agent up to the ℓth iteration, and $\hat{x}(\ell)$ is the best position among all the agents up to the ℓth iteration. Other PSO variants (e.g., [31], [32]) may be used.

CNO is proven to be almost surely convergent to the global optima of optimization problems [22].

III. Problem Formulation

A power consumption function of chillers is developed in [10], [33] as follows: For chiller i $(i = 1, 2, \ldots, n)$,

$$P_i(PLR_i) = a_i PLR_i^3 + b_i PLR_i^2 + c_i PLR_i + d_i \tag{6}$$

where n is the number of chillers, P_i is the power consumption of the ith chiller, $PLR_i \in [0, 1]$ is its partial load ratio, and a_i, b_i, c_i, and d_i are its coefficients. It is validated via experimentation that the cubic function is more realistic than the quadratic function where $a_i \equiv 0$ [34]. Note that the objective function in (6) is nonconvex if the second derivative of P_i with respect to PLR_i is negative for some i (i.e.,

This article has been accepted for publication in a future issue of this journal, but has not been fully edited. Content may change prior to final publication. Citation information: DOI 10.1109/TII.2022.3180080, IEEE Transactions on Industrial Informatics

$\exists i, 6a_i PLR_i + 2b_i < 0)\ \forall PLR_i \in [0,1]$. Namely, the objective function is nonconvex if $\exists i, b_i < \max\{0, -3a_i\}$.

Consider the following OCL problem formulation in [9]–[16], [34]–[36]:

$$\begin{aligned} \min_{PLR} \ & \sum_{i=1}^{n} P_i(PLR_i) \\ \text{subject to} \ & \sum_{i=1}^{n} \overline{P}_i PLR_i - P_D = 0, \\ & \underline{PLR}_i \le PLR_i \le \overline{PLR}_i,\ \forall i = 1, \dots, n, \end{aligned} \tag{7}$$

where $\overline{P}_i$ is the given nominal capacity of the ith chiller in the unit of refrigeration ton (RT), P_D is the demanded load in RT (1.0 RT $\approx$ 3.5 kW), and $\underline{PLR}_i \in [0,1)$ and $\overline{PLR}_i \in (0,1]$ are lower and upper bounds of PLR_i, respectively. The first and second constraints in (7) are a supply-demand constraint and a capacity constraint, respectively.

As aforementioned, for meeting some low demanded loads, it is not necessary to turn on all chillers simultaneously. To confine the number of chillers, the cardinality constraint is defined as follows:

$$\|PLR\|_0 \le k, \tag{8}$$

where $\|P$
elements
chillers to
$k \in [\mathrm{mi}$
largest ele
between
specific sc

In view
is introduced to denote the "off" or "on" status of chil
Consequently, the cardinality constraint in (8) and capa
constraint in (7) are reformulated as follows:

```
h=[y.*(1-y);
   sum(p.*C1(:,7))-P_D]; %对应TII论文公式（11）的等式约束，即 y(y-1)=0; sum(p.*C1(:,7))-P_D=0
dh=[zeros(nP,ny),C1(:,7);
   diag(1-2*y),zeros(ny,1)];
```

```
g1=sum(y)-K;
g=[g1]; %对应TII论文公式（8）的等式约束，即 ||PLR||0 <= k 即sum(y) <= K
dg=[zeros(nP,1);
   ones(ny,1)];
```

$$\sum_{i=1}^{n} y_i \le k, \quad \underline{PLR}_i y_i \le PLR_i \le \overline{PLR}_i y_i. \tag{9}$$

In contrast to the problem formulation with binary variables in its objective function as well as a constraint [11], the binary variables herein appear in the constraints only.

The binary variables can be realized by using the following quadratic equation as in [23], [27]:

$$y_i(y_i - 1) = 0, \quad \forall i = 1, \dots, n. \tag{10}$$

The cardinality-constrained OCL problem is then reformulated as follows:

$$\begin{aligned} \min_{PLR,y} \ & \sum_{i=1}^{n} P_i(PLR_i) \\ \text{subject to} \ & \sum_{i=1}^{n} \overline{P}_i PLR_i - P_D = 0, \\ & \underline{PLR}_i y_i \le PLR_i \le \overline{PLR}_i y_i, \\ & \sum_{i=1}^{n} y_i \le k,\ y_i(y_i - 1) = 0,\ \forall i = 1, \dots, n. \end{aligned} \tag{11}$$

As there are nonlinear equality constraints and a possibly nonconvex objective function in the reformulated OCL problem (11), it is a global optimization problem with a nonconvex feasible region and a possibly nonconvex objective function.

The cardinality constraint may be omitted solely from the power consumption minimization viewpoint. Nevertheless, the problem reformulation without the cardinality constraint may result in switching on more chillers than needed to meet a given demand, incurring higher maintenance costs. In addition, the feasible region without the cardinality constraint is substantially larger, entailing an increase in computational burden for optimization.

IV. A CNO-based Algorithm

A CNO-based optimal chiller loading (CNO-CL) algorithm is customized for solving problem (11). With the chiller parameters as its input data, it outputs the optimal partial load ratios and resulting wattage. Specifically, the chiller model parameters include the power consumption function coefficients and nominal capacities of the chiller systems and the bounds of PLR_i.

CNO-CL consists of two major components (i.e., PNNs and PSO) and two hyperparameters (i.e., the number of PNNs N and the minimal number of consecutive iterations at an
nd M depend on the
y. Large values of N
ms and vice versa. In
N and M are needed

values may be determined by using an experimental design method (e.g., the grid search method in [37] or Taguchi's design method in [38]) based on Monte Carlo test results.

Algorithm 1 describes the CNO-CL procedure. In Step 1, N and M are set. The termination counter m is set as 0. The initial states $x_i(0)$ and velocities $v_i(0)$ are randomly set. The individual minima $\tilde{x}_i(0)$ are set as the same values of initial states $x_i(0)$. The group minimum $\hat{x}^\star$ is set as the minimal state among all individual minima $\tilde{x}_i(0)$. In Steps 3-10, $\tilde{x}_i(\ell)$ is obtained as the best solution among the equilibria $\overline{x}_i(\ell)$ of the PNNs (4) up to the ℓth iteration. In Steps 11-17, the group minimum $\hat{x}^\star$ and the termination counter m are updated. In Steps 18-20, $v_i(\ell+1)$ and $x_i(\ell+1)$ are updated by using the PSO rule (5) to reinitialize the searching process. The optimization process continues until the termination counter m reaches a given termination criterion M.

V. Experimental Results

In this section, extensive experimental results are elaborated to evaluate the OCL performance of the proposed CNO-

This article has been accepted for publication in a future issue of this journal, but has not been fully edited. Content may change prior to final publication. Citation information: DOI 10.1109/TII.2022.3180080, IEEE Transactions on Industrial Informatics

Algorithm 1: CNO-CL

Input: The parameters of the chiller model.
Output: Optimal solution: $\hat{x}^\star$, $f(\hat{x}^\star)$.

Initialization: The number of PNNs N, the termination criterion M, the termination counter $m \leftarrow 0$, the PNN initial states $x_i(0)$ and velocities $v_i(0)$ for $i = 1, \ldots, N$; the individual minimum $\tilde{x}_i(0) \leftarrow x_i(0)$ for $i = 1, \ldots, N$; the group minimum $\hat{x}^\star \leftarrow \arg\min_{x_i}\{f(\tilde{x}_1(0)), \ldots, f(\tilde{x}_N(0))\}$, the PSO rule parameters c_0, c_1 and c_2.

```
while m ≤ M do
    for i = 1 to N do
        Compute the equilibrium states x̄_i(ℓ) by using
          PNN (4);
        if f(x̄_i(ℓ)) < f(x̃_i(ℓ − 1)) then
            x̃_i(ℓ) ← x̄_i(ℓ);
        else
            x̃_i(ℓ) ← x̃_i(ℓ);
        end
    end
    x* = arg min_{x_i(ℓ)} {f(x̃_1(ℓ)), ..., f(x̃_N(ℓ))};
    if f(x*) < f(x̂*) then
        x̂* ← x*;
        m ← 0;
    else
        m ← m + 1;
    end
    for i = 1 to N do
        Compute velocities v_i(ℓ + 1) and states
          x_i(ℓ + 1) according to the PSO rule (5);
    end
    ℓ ← ℓ + 1;
end
return x̂*, f(x̂*).
```

CL algorithm and several baseline methods, based on the published data in the references for a four-chiller system in a hotel, a six-chiller system in a hospital, an eight-chiller system in a semiconductor factory, and a 20-chiller system based on fivefold the four-chiller system. The code of CNO-CL is available at Github[1]. Note that the existing HVAC systems in large buildings are equipped with 4-20 chillers. For example, there are six chillers in the International Commerce Center in Hong Kong [39], ten chillers[2] in the Pentagon, and 20 chillers[3] in Burj Khalifa in Dubai.

A. A Four-chiller System

Consider a four-chiller system in a hotel in Taipei with its power consumption function coefficients and nominal capacities listed in Table I [10]. The lower and upper bounds of PLR_i are 0.3 and 1.0, respectively. Note the power consumption functions for chillers #2 and #3 are nonconvex as the second derivatives of of $P_i(PLR_i)$ with respect to PLR_i are [-1727.306, 0) and [-14.462, 0) for $PLR_2 \in [0.3000, 0.4977)$ and $PLR_3 = [0.3000, 0.3006)$, respectively.

The CNO-CL parameters are set as follows. In the PNN (4), ϵ is set as 10^{-3}. In the PSO-based rule (5), c_0, c_1 and c_2 are set as 1.0, 0.5 and 0.5, respectively.

TABLE I
POWER CONSUMPTION FUNCTION COEFFICIENTS AND NOMINAL CAPACITIES OF THE FOUR CHILLERS [10]

Chiller	a_i	b_i	c_i	d_i	$\overline{P}_i$ (RT)
#1	512.53	-430.13	166.57	104.09	450
#2	1456.53	-2174.53	1177.79	-67.15	450
#3	-63.2	1151.42	-779.13	384.71	1000
#4	4021.41	-3626.5	413.48	541.63	1000

Fig. 1 snapshots the transient states of a PNN and the corresponding wattage with various values of α, β, and P_D (i.e., 2610 RT, 2320 RT, 2030 RT, and 1740 RT). It shows that the PNN is globally stable and reaches its equilibria in around 0.02 seconds. It also indicates that the result is robust to the different values of α and β. In the following experiments, α and β are set as 10. Fig. 2 illustrates Monte Carlo test results on power consumption using CNO-CL over 100 independent runs for P_D being 1450 RT and 1160 RT. It shows that CNO-CL reaches minimal power consumption levels if $N \geq 3$ and $M \geq 10$. As a larger value of M leads to a longer computation time, M is set as 10 in the four-chiller system. Fig. 3 depicts the CNO-CL convergent behaviors and the corresponding wattage for chiller loading with P_D being 1450 RT and 1160 RT. It shows that CNO-CL converges within ten iterations.

Table II summarizes the wattage obtained using CNO-CL in comparison with the results obtained by using six baseline methods. It shows that CNO-CL performs equally well as GAMS and outperforms almost all other baselines in terms of best, mean, and standard deviation (SD) of the objective function values. It also shows that the best results obtained by using CNO-CL are able to save up to 0.26%, 0.11%, 0.47%, 0.96%, 9.66%, and 23.97% of wattage; while meeting six demanded loads. It implies that CNO-CL is able to result in more savings than the baselines for lower demanded loads. Besides, it shows that the solution standard deviations obtained by using CNO-CL are zero, indicating the highest consistency of CNO-CL.

In view that GAMS consists of a set of exact methods, the results obtained by using GAMS are considered to be globally optimal. Table III records the details of the resulting operation status of the four-chiller system by using GAMS and CNO-CL. It shows that PLR_i and P_i obtained by using CNO-CL and GAMS are almost the same, with some very small discrepancies as underlined.

The first derivative of the objective function in (11) with respect to PLR_i is positive for the four-chiller system; i.e., $3a_iPLR_i^2 + 2b_iPLR_i + c_i > 0,\ i = 1, 2, 3, 4$. As such, the objective function is a monotone increasing function. As mentioned above, as the second derivative of the objective function is negative for chillers #2 and #3, the objective function is not convex. The combination of monotonicity and nonconvexity

[1] https://github.com/Jzzz-zy
[2] https://www.esmagazine.com/articles/85037-the-pentagon-8217-s-\ HVAC-attack
[3] https://www.designbuild-network.com/projects/burj/

This article has been accepted for publication in a future issue of this journal, but has not been fully edited. Content may change prior to final publication. Citation information: DOI 10.1109/TII.2022.3180080, IEEE Transactions on Industrial Informatics

implies that the objective function is pseudoconvex [40]. For some given load demands (e.g., $P_D \in \{2610$ RT, 2320 RT, 2030 RT, and 1740 RT$\}$), all chillers need to be switched on simultaneously (i.e., $y_i = 1, \forall i = 1, 2, 3, 4.$) to achieve optimal loading. As a result, the cardinality constraint in (11) is not active. As aforementioned, a single PNN is convergent to global optimal solutions of a pseudoconvex optimization problem [21]. The results in Fig. 1 and Table III echo the phenomenon.

B. A Six-chiller System

Consider a six-chiller system in a hospital in Kaohsiung with its coefficients and nominal capacities listed in Table IV [35]. The lower bounds of PLR_i are 0.3 and 0.5 for chillers #1-#4 and chillers #5-#6, respectively. The upper bound is 1.0 for all chillers. Note the power consumption functions for chillers #2, #3, #4, and #6 are nonconvex because the second derivatives of $P_i(PLR_i)$ are in [-110.15, 0), [-884.27, 0), [-538.32, -1114.14], and [-968.89, 0) for $PLR_2 \in [0.3000, 0.5404]$, $PLR_3 \in [0.3000, 0.7963]$, $PLR_4 \in [0.3, 1.0]$, and $PLR_6 \in [0.5000, 0.6906]$, respectively. The parameter setting (except M and N) is the same as that in the four-chiller system.

Fig. 4 illustrates Monte Carlo test results on power consumption using CNO-CL over 100 independent runs for P_D being 4080 RT, 3570 RT, 3060 RT, 2550 RT, 2040 RT, and 1530 RT. It shows that CNO-CL reaches the minimal power consumption if $N \geq 3$ and $M \geq 10$. M is set as 10 in the six-chiller system to record computation time. Fig. 5 depicts the convergent behaviors of CNO-CL and corresponding wattage for optimal chiller loading in the six-chiller system. It also shows that CNO-CL converges within ten iterations.

Table V records the detailed operating status and wattage obtained by using CNO-CL. Table VI summarizes the statistics of wattage and average computation time by using CNO-CL and baseline methods over 100 independent runs. The algorithms of the baselines are coded by customizing the codes provided by Yarpiz[4] in MATLAB Central[5]. Table VI shows that CNO-CL always results in minimal power consumption, outperforming almost all baselines in terms of the best, mean, and standard deviation of the objective function values. It also shows that the loading solutions obtained by using CNO-CL are able to save, on average, 0.75%-2.71%, 1.32%-3.98%, 1.09%-4.70%, 0.22%-7.04%, 1.82%-7.86%, and 1.77%-9.56% of wattage; while meeting the six load demands. It implies that CNO-CL is able to achieve more savings than the baselines for lower demanded loads. In addition, it shows that all the standard deviations of the solutions obtained by using CNO-CL are zero, indicating the highest consistency of CNO-CL among the baselines. Besides, Table VI records the average computation time spent by the competing methods in the same computing environment. It shows that the average time spent by CNO-CL to obtain optimal solutions is around 1.5-2.5 seconds in the six-chiller system.

[4]www.yarpiz.com

[5]https://ww2.mathworks.cn/matlabcentral/fileexchange/?q=profileid:6876387

C. An Eight-chiller System

Consider an eight-chiller system in a semiconductor factory in Hsinchu Science Industrial District with its parameters listed in Table VII [9]. The lower and upper bounds of PLR_i are 0.5 and 1.0, respectively. Note that the power consumption functions for chillers #1 and #6 are nonconvex because the second derivatives of $P_1(PLR_1)$ and $P_6(PLR_6)$ are [-328.53, 0) and [-112.77, 0) for $PLR_1 \in [0.5000, 0.7165)$ and $PLR_6 \in [0.5000, 0.5248)$, respectively. As such, the objective function of the problem (11) is also nonconvex. The parameter setting (except M and N) is the same as in subsection V-A.

Fig. 6 illustrates Monte Carlo test results on power consumption using CNO-CL over 100 independent runs with P_D being 8000 RT, 7000 RT, 6000 RT, 5000 RT, 4000 RT, and 3000 RT. It shows that CNO-CL reaches the minimal power consumption if $N \geq 4$ and $M \geq 10$. To ensure a high computation efficiency, M is set as 10 in the eight-chiller system. Fig. 7 depicts the convergent behaviors of CNO-CL and corresponding wattage for the eight-chiller system. It shows that CNO-CL also converges within ten iterations.

Table VIII records the detailed operating status and power consumption obtained by using CNO-CL for the eight-chiller system. Table IX summarizes the statistics of wattage and average computation time using CNO-CL and four competing baselines over 100 independent runs. It shows that CNO-CL always results in the lowest wattage, outperforming almost all baselines in terms of minimal wattage, mean wattage, and standard deviation. It also shows that the mean wattage minimized by using CNO-CL brings 0.04%-8.00%, 3.74%-11.08%, 3.61%-12.85%, 1.25%-14.59%, 3.13%-18.83%, and 1.04%-23.85% of savings; while meeting the six demands. It implies that CNO-CL is able to achieve more savings than the baselines, especially for lower cooling loads. In addition, the standard deviations of solutions obtained by using CNO-CL are also zero, indicating the highest consistency of CNO-CL. Besides, the average time is around 3-5 seconds for CNO-CL to converge in the eight-chiller system.

D. A 20-chiller System

Consider a 20-chiller system by quintupling the data of the four-chiller system in subsection V-A, where k is set as 20, 20, 20, 18, 13, and 11, for P_D being 13050 RT, 11600 RT, 10150 RT, 8700 RT, 7250 RT, and 5800 RT, respectively. All parameters in CNO-CL, except N, are set as the same as those in subsection V-A. Similar to the preceding subsections, N is selected based on Monte Carlo tests as 1, 2, 2, 20, 40, and 40 for the six demanded loads.

Table X records the detailed operating status and power consumption obtained by using CNO-CL for the 20-chiller system. As shown in the table, all chillers are switched on to meet P_D with three higher values (i.e., 13050 RT, 11600 RT, and 10150 RT), the same as the four-chiller system for its three higher P_D (i.e., 2610 RT, 2320 RT, and 2030 RT). Note that, to meet their three higher P_D values, the power consumption in the 20-chiller system equals the fivefold power consumption in the four-chiller system, respectively. The results in the table also show that, for three lower P_D values (i.e., 8700 RT,

This article has been accepted for publication in a future issue of this journal, but has not been fully edited. Content may change prior to final publication. Citation information: DOI 10.1109/TII.2022.3180080, IEEE Transactions on Industrial Informatics

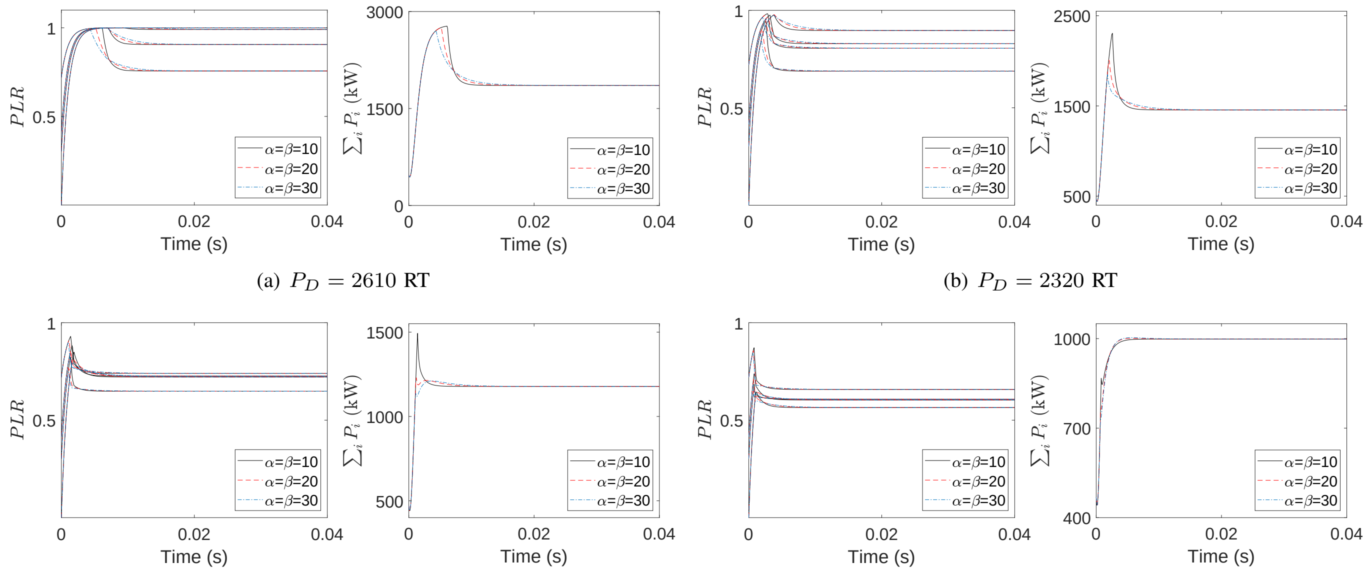

(a) $P_D = 2610$ RT (b) $P_D = 2320$ RT

(c) $P_D = 2030$ RT (d) $P_D = 1740$ RT

Fig. 1. Snapshots of the PNN transient states in CNO-CL for the four-chiller system with various values of α and β, where $k = 4$.

TABLE II
STATISTICS OF RESULTING POWER CONSUMPTION (KW) FOR THE FOUR-CHILLER SYSTEM USING CNO-CL AND SIX BASELINES

Method	P_D=2610 RT				P_D=2320 RT				P_D=2030 RT			
	best	worst	mean	SD	best	worst	mean	SD	best	worst	mean	SD
GAMS [11]	**1857.30**	-	-	-	**1455.66**	-	-	-	**1178.14**	-	-	-
GA [10]	1862.18	-	-	-	1457.23	-	-	-	1183.80	-	-	-
LGM [10]	**1857.30**	1864.17	-	-	**1455.66**	1461.05	-	-	**1178.14**	1182.50	-	-
PSO [13]	**1857.30**	1857.45	1857.43	0.04	**1455.66**	1522.42	1462.34	20.03	**1178.14**	**1178.14**	**1178.14**	**0.00**
DE [14]	**1857.30**	1858.57	1857.43	0.40	**1455.66**	**1455.66**	**1455.66**	**0.00**	**1178.14**	**1178.14**	**1178.14**	**0.00**
DCSA [16]	**1857.30**	1857.40	1857.32	0.02	1455.67	1458.48	1455.81	0.53	**1178.14**	1199.50	1181.07	4.80
CNO-CL	**1857.30**	**1857.30**	**1857.30**	**0.00**	**1455.66**	**1455.66**	**1455.66**	**0.00**	**1178.14**	**1178.14**	**1178.14**	**0.00**
Method	P_D=1740 RT				P_D=1450 RT				P_D=1160 RT			
	best	worst	mean	SD	best	worst	mean	SD	best	worst	mean	SD
GAMS [11]	**998.53**	-	-	-	**820.07**	-	-	-	**651.07**	-	-	-
GA [10]	1001.62	-	-	-	907.72	-	-	-	856.30	-	-	-
LGM [10]	**998.53**	1002.22	-	-	904.62	907.97	-	-	849.99	853.13	-	-
PSO [13]	**998.53**	1013.43	1005.36	5.71	**820.07**	847.53	826.52	10.88	**651.07**	691.19	667.12	19.65
DE [14]	**998.53**	1009.20	1000.21	3.66	**820.07**	821.28	820.19	0.38	**651.07**	655.63	651.53	1.44
DCSA [16]	1008.24*	1074.55*	1038.13*	25.72	825.72*	897.06*	838.05*	17.43	652.16*	794.25*	713.17*	44.02
CNO-CL	**998.53**	**998.53**	**998.53**	**0.00**	**820.07**	**820.07**	**820.07**	**0.00**	**651.07**	**651.07**	**651.07**	**0.00**

* In [16], P_i is negative and thus infeasible for PLR_i being near 0.0000. The wattage here is corrected by setting $P_i = 0$.

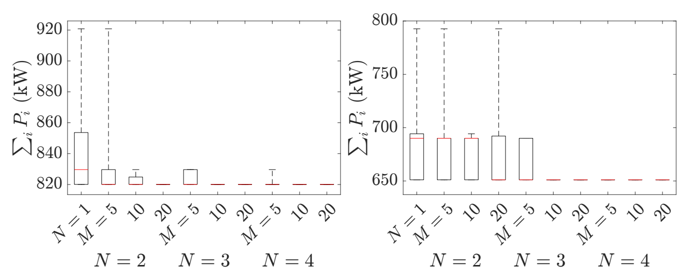

(a) $P_D = 1450$ RT, $k = 3$ (b) $P_D = 1160$ RT, $k = 2$

Fig. 2. Boxplots of wattage resulted from the Monte Carlo tests using CNO-CL with various values of N and M in the four-chiller system.

7250 RT, and 5800 RT), the number of active chillers in the 20-chiller system is not the same as the fivefold of active chillers in the four-chiller system for their three lower P_D values (i.e., 1740 RT, 1450 RT, and 1160 RT), because the number of chiller combinations in the 20-chiller system is much more than the fivefold in the four-chiller system. As a result of the much enlarged feasible region for optimization, the power consumption for three lower P_D values in the 20-chiller system is less than the fivefold power consumption in the four-chiller system for their three lower P_D values, respectively.

Table XI summarizes the statistics of wattage and computation time using CNO-CL and the baselines over 100 independent runs. It shows that CNO-CL always results in the lowest wattage and standard deviation. It also indicates that the mean wattage minimized by using CNO-CL brings 0.01%-13.59%, 0.00%-20.45%, 0.10%-21.02%, 0.56%-21.36%, 2.53%-21.08%, and 3.72%-19.65% of savings com-

This article has been accepted for publication in a future issue of this journal, but has not been fully edited. Content may change prior to final publication. Citation information: DOI 10.1109/TII.2022.3180080, IEEE Transactions on Industrial Informatics

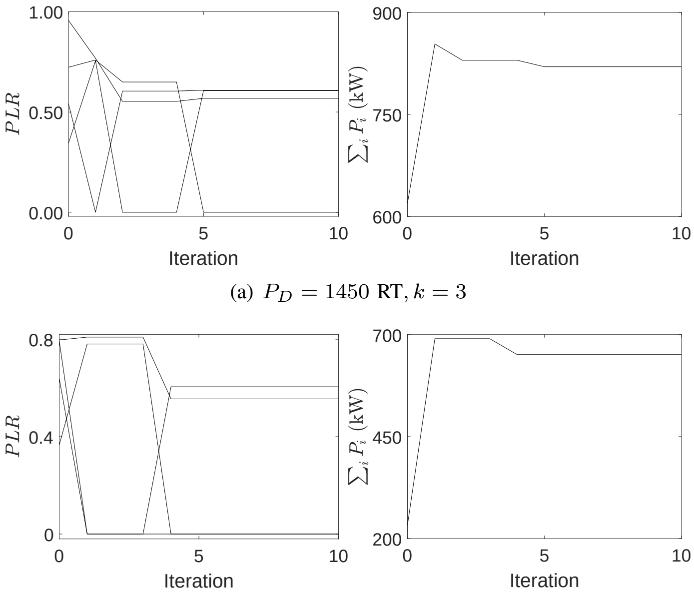

(a) $P_D = 1450$ RT, $k = 3$

(b) $P_D = 1160$ RT, $k = 2$

Fig. 3. Convergent behavior and corresponding wattage by using CNO-CL in the four-chiller system, where $N = 3$.

TABLE III
RESULTING OPERATION STATUS OF THE FOUR-CHILLER SYSTEM USING GAMS [11] AND CNO-CL

P_D (RT)	chiller	status	PLR_i	P_i (kW)		$\sum_{i=1}^{4} P_i$ (kW)
				GAMS	CNO -CL	
2610	#1	on	0.99	345.42	345.43	1857.30
	#2	on	0.91	298.11	298.07	
	#3	on	1.00	693.80	693.80	
	#4	on	0.76	519.98	519.99	
2320	#1	on	0.83	238.48	238.52	1455.66
	#2	on	0.81	231.98	231.92	
	#3	on	0.90	566.18	566.19	
	#4	on	0.69	419.03	419.04	
2030	#1	on	0.73	194.53	194.50	1178.14
	#2	on	0.74	203.96	203.94	
	#3	on	0.72	398.26	398.28	
	#4	on	0.65	381.39	381.42	
1740	#1	on	0.60	160.68	160.62	998.53
	#2	on	0.66	181.22	181.22	
	#3	on	0.56	300.58	300.57	
	#4	on	0.61	356.06	356.13	
1450	#1	on	0.61	161.31	161.30	820.07
	#2	off	0.00	0.00	0.00	
	#3	on	0.57	302.18	302.19	
	#4	on	0.61	356.58	356.58	
1160	#1	off	0.00	0.00	0.00	651.07
	#2	off	0.00	0.00	0.00	
	#3	on	0.56	296.19	296.19	
	#4	on	0.60	354.88	354.89	

pared with the baselines for the six different P_D values. Moreover, the average computation time is lowest for P_D with three bigger values. In particular, the average computation time for P_D being 13050 RT is less than one second. The average computation time for other demanded loads is much smaller than dispatching intervals (e.g., 15 minutes [6]).

VI. Concluding Remarks

In this paper, optimal chiller loading in HVAC systems is formulated as a cardinality-constrained global optimization problem. A CNO-based approach is proposed for optimal chiller loading by solving the formulated problem. The experimental results based on published chiller system model parameters show that the CNO-CL method with several projection neural networks is capable of optimal chiller loading with the minimum wattage and outperforms all meta-heuristic baselines. Further investigations along this line of research may include dynamic optimal chiller loading and multi-scale optimization and control of HVAC systems.

TABLE IV
POWER CONSUMPTION FUNCTION COEFFICIENTS AND NOMINAL CAPACITIES OF THE SIX CHILLERS [35]

Chiller	a_i	b_i	c_i	d_i	$\overline{P}_i$ (RT)
#1	7.85	0.05	329.73	57.2	550
#2	76.36	-123.8	419.28	50.09	550
#3	296.93	-709.37	1226.94	-76.29	1000
#4	-137.1	-145.77	1100.42	-72.56	1000
#5	59.33	-28.24	620.62	69.39	1000
#6	847.43	-1755.59	1817.08	-186.18	1000

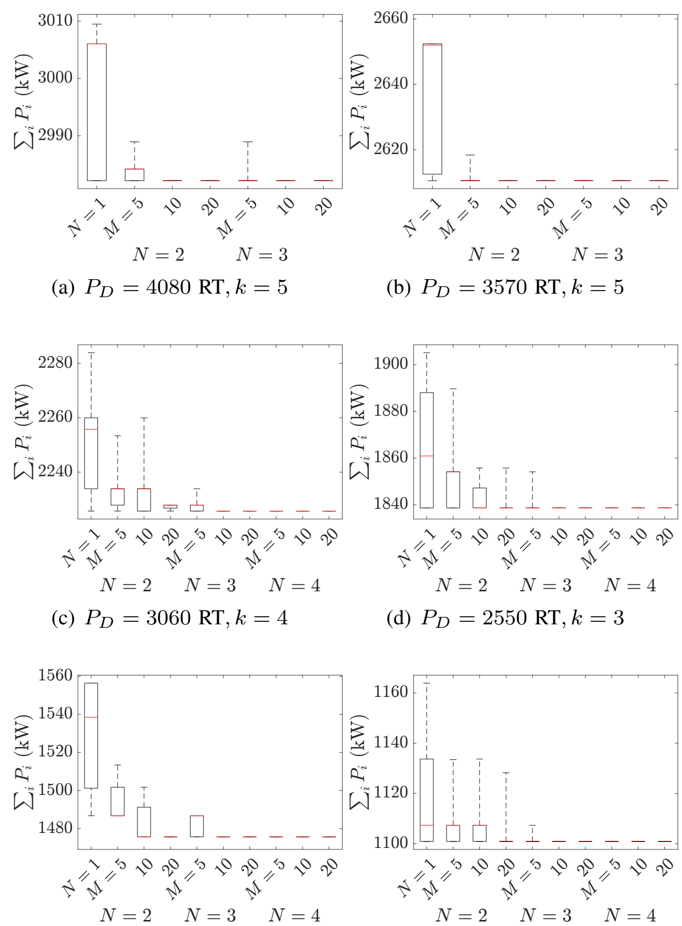

(a) $P_D = 4080$ RT, $k = 5$ (b) $P_D = 3570$ RT, $k = 5$

(c) $P_D = 3060$ RT, $k = 4$ (d) $P_D = 2550$ RT, $k = 3$

(e) $P_D = 2040$ RT, $k = 3$ (f) $P_D = 1530$ RT, $k = 2$

Fig. 4. Boxplots of wattage resulted from the Monte Carlo tests using CNO-CL with various values of N and M in the six-chiller system.

References

[1] N. K. Dhar, N. K. Verma, and L. Behera, "Adaptive critic-based event-triggered control for HVAC system," *IEEE Trans. Ind. Informat.*, vol. 14, no. 1, pp. 178–188, 2017.

This article has been accepted for publication in a future issue of this journal, but has not been fully edited. Content may change prior to final publication. Citation information: DOI 10.1109/TII.2022.3180080, IEEE Transactions on Industrial Informatics

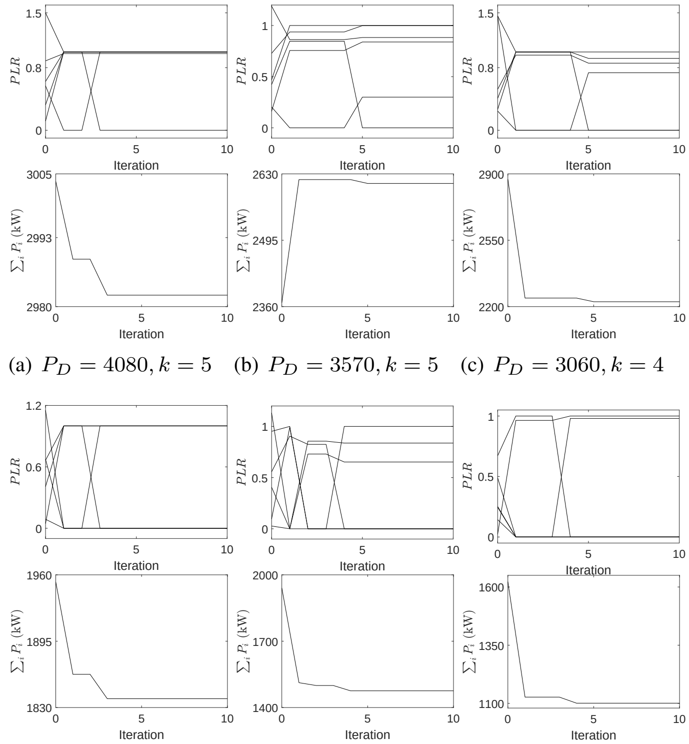

(a) $P_D = 4080, k = 5$ (b) $P_D = 3570, k = 5$ (c) $P_D = 3060, k = 4$

(d) $P_D = 2550, k = 3$ (e) $P_D = 2040, k = 3$ (f) $P_D = 1530, k = 2$

Fig. 5. Convergent behavior and corresponding wattage by using CNO-CL in the six-chiller system, where $N = 3$.

TABLE V
RESULTING OPERATION STATUS OF THE SIX-CHILLER SYSTEM USING CNO-CL

P_D	chiller		status		PLR_i		P_i (kW)		$\sum_{i=1}^{6} P_i$ (kW)
4080	#1	#2	on	on	1.00	1.00	394.83	421.93	2982.15
	#3	#4	on	off	1.00	0.00	738.21	0.00	
	#5	#6	on	on	1.00	0.98	721.10	706.08	
3570	#1	#2	on	off	1.00	0.00	394.83	0.00	2610.55
	#3	#4	on	on	1.00	0.30	737.23	240.74	
	#5	#6	on	on	0.84	0.88	605.13	632.61	
3060	#1	#2	on	off	1.00	0.00	394.83	0.00	2225.68
	#3	#4	on	off	0.92	0.00	681.98	0.00	
	#5	#6	on	on	0.73	0.86	533.77	615.10	
2550	#1	#2	on	off	1.00	0.00	394.83	0.00	1838.67
	#3	#4	off	off	0.00	0.00	0.00	0.00	
	#5	#6	on	on	1.00	1.00	721.10	722.74	
2040	#1	#2	on	off	1.00	0.00	394.83	0.00	1475.68
	#3	#4	off	off	0.00	0.00	0.00	0.00	
	#5	#6	on	on	0.65	0.84	478.87	601.98	
1530	#1	#2	on	off	1.00	0.00	394.83	0.00	1100.91
	#3	#4	off	off	0.00	0.00	0.00	0.00	
	#5	#6	off	on	0.00	0.98	0.00	706.08	

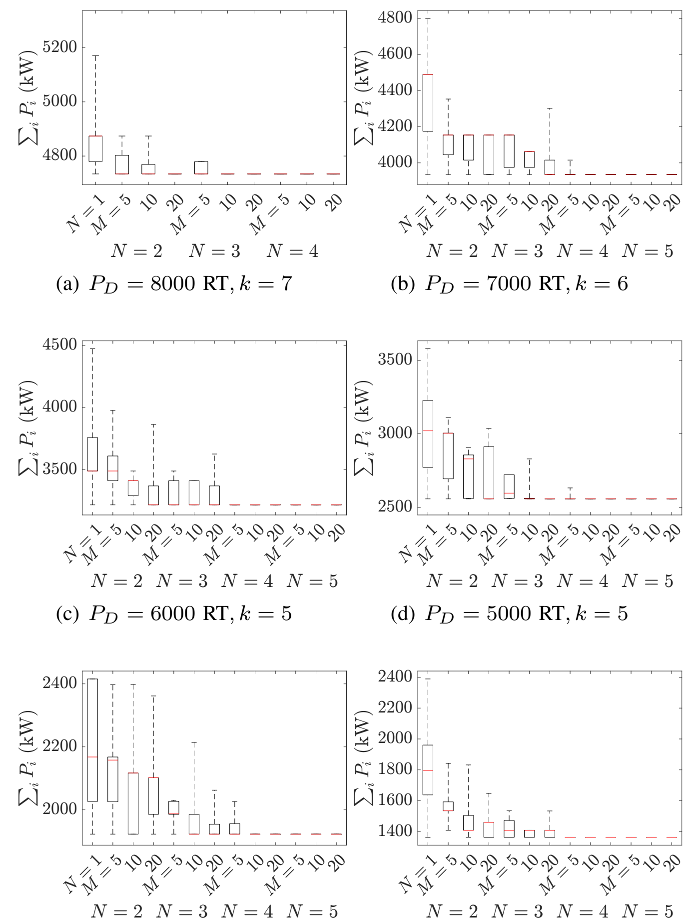

(a) $P_D = 8000$ RT, $k = 7$ (b) $P_D = 7000$ RT, $k = 6$

(c) $P_D = 6000$ RT, $k = 5$ (d) $P_D = 5000$ RT, $k = 5$

(e) $P_D = 4000$ RT, $k = 4$ (f) $P_D = 3000$ RT, $k = 3$

Fig. 6. Boxplots of wattage resulted from the Monte Carlo tests using CNO-CL with various values of N and M in the eight-chiller system.

[2] A. Jindal, N. Kumar, and J. J. Rodrigues, "A heuristic-based smart HVAC energy management scheme for university buildings," *IEEE Trans. Ind. Informat.*, vol. 14, no. 11, pp. 5074–5086, 2018.

[3] K. Ma, Y. Yu, B. Yang, and J. Yang, "Demand-side energy management considering price oscillations for residential building heating and ventilation systems," *IEEE Trans. Ind. Informat.*, vol. 15, no. 8, pp. 4742–4752, 2019.

[4] E. Rezaei and H. Dagdougui, "Optimal real-time energy management in apartment building integrating microgrid with multizone HVAC control," *IEEE Trans. Ind. Informat.*, vol. 16, no. 11, pp. 6848–6856, 2020.

[5] Y.-C. Chang, "Optimal chiller loading by evolution strategy for saving energy," *Energy Build.*, vol. 39, no. 4, pp. 437–444, 2007.

[6] D. Zhang, P. B. Luh, J. Fan, and S. Gupta, "Chiller plant operation optimization: Energy-efficient primary-only and primary–secondary systems," *IEEE Trans. Autom. Sci. Eng.*, vol. 15, no. 1, pp. 341–355, 2017.

[7] F. Oliveira and A. Ukil, "Comparative performance analysis of induction and synchronous reluctance motors in chiller systems for energy efficient buildings," *IEEE Trans. Ind. Informat.*, vol. 15, no. 8, pp. 4384–4393, 2019.

[8] Y.-C. Chang, C.-Y. Lee, C.-R. Chen, C.-J. Chou, W.-H. Chen, and W.-H. Chen, "Evolution strategy based optimal chiller loading for saving energy," *Energy Convers. Manag.*, vol. 50, no. 1, pp. 132–139, 2009.

[9] Y.-C. Chang and H.-C. Tu, "An effective method for reducing power consumption-optimal chiller load distribution," in *Proc. Int. Conf. on Power Syst. Tech.*, vol. 2. IEEE, 2002, pp. 1169–1172.

[10] Y.-C. Chang, J.-K. Lin, and M.-H. Chuang, "Optimal chiller loading by genetic algorithm for reducing energy consumption," *Energy Build.*, vol. 37, no. 2, pp. 147–155, 2005.

[11] E. Salari and A. Askarzadeh, "A new solution for loading optimization of multi-chiller systems by general algebraic modeling system," *Appl. Therm. Eng.*, vol. 84, pp. 429–436, 2015.

[12] A. J. Ardakani, F. F. Ardakani, and S. Hosseinian, "A novel approach for optimal chiller loading using particle swarm optimization," *Energy Build.*, vol. 40, no. 12, pp. 2177–2187, 2008.

[13] W.-S. Lee and L.-C. Lin, "Optimal chiller loading by particle swarm algorithm for reducing energy consumption," *Appl. Therm. Eng.*, vol. 29, no. 8-9, pp. 1730–1734, 2009.

[14] W.-S. Lee, Y.-T. Chen, and Y. Kao, "Optimal chiller loading by differential evolution algorithm for reducing energy consumption," *Energy Build.*, vol. 43, no. 2-3, pp. 599–604, 2011.

[15] L. dos Santos Coelho and V. C. Mariani, "Improved firefly algorithm approach applied to chiller loading for energy conservation," *Energy Build.*, vol. 59, pp. 273–278, 2013.

[16] L. dos Santos Coelho, C. E. Klein, S. L. Sabat, and V. C. Mariani, "Optimal chiller loading for energy conservation using a new differential

TABLE VI
STATISTICS OF RESULTING POWER CONSUMPTION (KW) AND COMPUTATION TIME (SECONDS) FOR THE SIX-CHILLER SYSTEM USING CNO-CL AND FOUR BASELINES

Method	P_D=4080 RT				P_D=3570 RT				P_D=3060 RT			
	best / worst	mean	SD	average time	best / worst	mean	SD	average time	best / worst	mean	SD	average time
GA [12]	3002.48 / 3080.04	3051.41	16.51	3.64	2652.79 / 2733.84	2690.37	15.61	3.42	2281.31 / 2391.24	2335.34	20.26	3.39
PSO [12]	**2982.15** / 3053.28	3004.75	13.61	**1.32**	2617.29 / 2675.91	2645.47	17.19	**1.24**	2226.46 / 2315.43	2250.23	16.42	**1.18**
DE [14]	3008.38 / 3106.96	3065.37	18.31	2.76	2645.28 / 2784.49	2718.82	33.35	2.83	2242.21 / 2429.14	2309.57	51.94	2.68
IFA [15]	2984.21 / 3053.09	3013.61	14.22	16.24	2611.16 / 2678.05	2661.03	11.91	15.55	2245.24 / 2347.62	2294.24	25.38	15.25
CNO-CL	**2982.15/ 2982.15**	**2982.15**	**0.00**	2.09	**2610.55 / 2610.55**	**2610.55**	**0.00**	2.32	**2225.68 / 2225.68**	**2225.68**	**0.00**	2.47
Method	P_D=2550 RT				P_D=2040 RT				P_D=1530 RT			
	best / worst	mean	SD	average time	best / worst	mean	SD	average time	best / worst	mean	SD	average time
GA [12]	1913.82 / 2029.16	1977.87	24.85	3.39	1518.30 / 1651.93	1601.51	23.27	3.59	1158.77 / 1284.01	1217.25	24.37	3.43
PSO [12]	**1838.67** / 1905.13	1861.80	18.68	**1.16**	**1475.68** / 1558.55	1503.02	18.12	**1.19**	**1100.91** / 1152.48	1120.71	15.53	**1.16**
DE [14]	**1838.67** / 1854.14	1842.69	6.82	2.60	1482.34 / 1664.87	1525.33	37.45	2.64	1100.94 / 1321.54	1159.24	42.72	2.70
IFA [15]	1853.92 / 1971.80	1926.22	26.96	15.20	1486.83 / 1617.98	1547.35	26.91	15.19	1107.35 / 1215.08	1170.71	26.48	15.15
CNO-CL	**1838.67 / 1838.67**	**1838.67**	**0.00**	1.59	**1475.68 / 1475.68**	**1475.68**	**0.00**	2.31	**1100.91 / 1100.91**	**1100.91**	**0.00**	2.15

TABLE VII
POWER CONSUMPTION FUNCTION COEFFICIENTS AND NOMINAL CAPACITIES OF THE EIGHT CHILLERS [9]

Chiller	a_i	b_i	c_i	d_i	$\overline{P_i}$ (RT)
#1	252.91	-543.63	840.18	-13.17	1250
#2	1265.94	-1602.73	1006.97	150.06	1250
#3	2105.48	-2341.48	1339.36	171.91	1250
#4	701.45	-222.59	568.12	202.08	1250
#5	3.12	343.24	142.53	195.03	1250
#6	757.47	-1192.59	1339.29	-21.21	1250
#7	347.75	-358.39	418.92	139.03	1250
#8	678.46	-715.28	980.13	45.61	1250

TABLE VIII
RESULTING OPERATION STATUS OF THE EIGHT-CHILLER SYSTEM USING CNO-CL

P_D (RT)	chiller		status		PLR_i		P_i (kW)		$\sum_{i=1}^{8} P_i$ (kW)
8000	#1	#2	on	on	1.00	0.89	536.29	674.80	4734.01
	#3	#4	on	off	0.71	0.00	690.76	0.00	
	#5	#6	on	on	1.00	0.98	683.92	856.13	
	#7	#8	on	on	1.00	0.82	547.31	744.80	
7000	#1	#2	on	on	1.00	0.87	536.29	651.76	3935.19
	#3	#4	off	off	0.00	0.00	0.00	0.00	
	#5	#6	on	on	1.00	0.94	683.92	815.18	
	#7	#8	on	on	1.00	0.78	547.31	700.73	
6000	#1	#2	on	on	1.00	0.87	536.29	645.33	3216.29
	#3	#4	off	off	0.00	0.00	0.00	0.00	
	#5	#6	on	on	1.00	0.93	683.92	803.44	
	#7	#8	on	off	1.00	0.00	547.31	0.00	
5000	#1	#2	on	on	1.00	0.73	536.29	525.88	2557.33
	#3	#4	off	off	0.00	0.00	0.00	0.00	
	#5	#6	on	off	0.80	0.00	531.42	0.00	
	#7	#8	on	on	0.97	0.50	522.08	441.663	
4000	#1	#2	on	on	1.00	0.68	536.29	493.30	1922.78
	#3	#4	off	off	0.00	0.00	0.00	0.00	
	#5	#6	on	off	0.64	0.00	430.06	0.00	
	#7	#8	on	off	0.87	0.00	463.14	0.00	
3000	#1	#2	on	off	1.00	0.00	536.29	0.00	1363.33
	#3	#4	off	off	0.00	0.00	0.00	0.00	
	#5	#6	on	off	0.57	0.00	390.20	0.00	
	#7	#8	on	off	0.83	0.00	436.83	0.00	

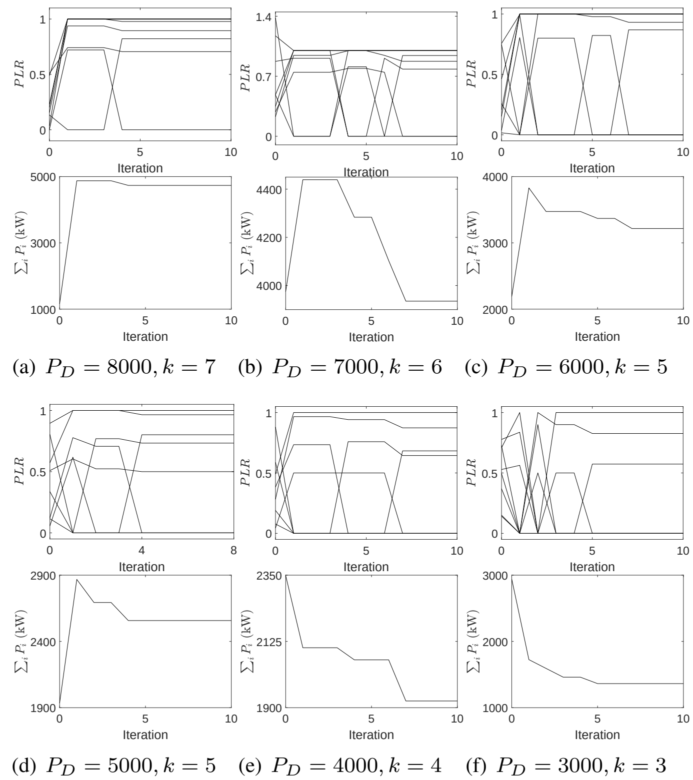

(a) $P_D = 8000, k = 7$ (b) $P_D = 7000, k = 6$ (c) $P_D = 6000, k = 5$

(d) $P_D = 5000, k = 5$ (e) $P_D = 4000, k = 4$ (f) $P_D = 3000, k = 3$

Fig. 7. Convergent behaviors and corresponding wattage by using CNO-CL in the eight-chiller system, where $N = 4$.

cuckoo search approach," *Energy*, vol. 75, pp. 237–243, 2014.

[17] Z. Zhao, S. Liu, M. Zhou, and A. Abusorrah, "Dual-objective mixed integer linear program and memetic algorithm for an industrial group scheduling problem," *IEEE/CAA J. Autom. Sinica*, vol. 8, no. 6, pp. 1199–1209, 2020.

[18] K. Deng, Y. Sun, S. Li, Y. Lu, J. Brouwer, P. G. Mehta, M. Zhou, and A. Chakraborty, "Model predictive control of central chiller plant with thermal energy storage via dynamic programming and mixed-integer linear programming," *IEEE Trans. Autom. Sci. Eng.*, vol. 12, no. 2, pp. 565–579, 2014.

[19] D. Tank and J. Hopfield, "Simple'neural'optimization networks: An A/D converter, signal decision circuit, and a linear programming circuit," *IEEE Trans. Circuits. Syst.*, vol. 33, no. 5, pp. 533–541, 1986.

[20] Y. Xia, H. Leung, and J. Wang, "A projection neural network and its application to constrained optimization problems," *IEEE Trans. Circuits and Systems: Part I*, vol. 49, no. 4, pp. 447–458, 2002.

[21] X. Hu and J. Wang, "Solving pseudomonotone variational inequalities and pseudoconvex optimization problems using the projection neural network," *IEEE Transactions on Neural Networks*, vol. 17, no. 6, pp. 1487–1499, 2006.

[22] Z. Yan, J. Fan, and J. Wang, "A collective neurodynamic approach to constrained global optimization," *IEEE Transactions on Neural Networks and Learning Systems*, vol. 28, no. 5, pp. 1206–1215, 2017.

[23] H. Che and J. Wang, "A collaborative neurodynamic approach to global and combinatorial optimization," *Neural Networks*, vol. 114, pp. 15 – 27, 2019.

[24] C. Xu and X. He, "A fully distributed approach to optimal energy scheduling of users and generators considering a novel combined neurodynamic algorithm in smart grid," *IEEE/CAA J. Autom. Sin.*, vol. 8, no. 7, pp. 1325–1335, 2021.

[25] E. L. Lawler and D. E. Wood, "Branch-and-bound methods: A survey," *Operations Research*, vol. 14, no. 4, pp. 699–719, 1966.

[26] T. Westerlund and F. Pettersson, "An extended cutting plane method for solving convex MINLP problems," *Comput. Chem. Eng.*, vol. 19, pp. 131–136, 1995.

This article has been accepted for publication in a future issue of this journal, but has not been fully edited. Content may change prior to final publication. Citation information: DOI 10.1109/TII.2022.3180080, IEEE Transactions on Industrial Informatics

TABLE IX
STATISTICS OF RESULTING POWER CONSUMPTION (KW) AND COMPUTATION TIME (SECONDS) FOR THE EIGHT-CHILLER SYSTEM USING CNO-CL AND FOUR BASELINES

Method	P_D=8000 RT				P_D=7000 RT				P_D=6000 RT			
	best / worst	mean	SD	average time	best / worst	mean	SD	average time	best / worst	mean	SD	average time
GA [12]	4753.76 / 4937.83	4820.09	41.49	4.89	4007.62 / 4306.64	4188.72	41.47	4.74	3405.03 / 3762.39	3625.51	104.95	4.75
PSO [12]	4734.77 / 5952.85	5022.53	256.79	**1.59**	3935.20 / 4736.15	4147.30	200.63	**1.58**	**3216.29** / 3976.31	3336.61	166.04	**1.58**
DE [14]	4834.23 / 5544.16	5145.81	157.69	4.27	4014.22 / 4997.32	4425.73	210.09	4.30	3273.93 / 4106.53	3690.33	204.26	4.29
IFA [15]	4735.71 / 4735.83	4735.75	0.02	28.21	3963.71 / 4112.02	4087.98	46.04	28.09	3296.50 / 3714.69	3486.36	114.06	28.06
CNO-CL	**4734.01 / 4734.01**	**4734.01**	**0.00**	3.31	**3935.19 / 3935.19**	**3935.19**	**0.00**	3.55	**3216.29 / 3216.29**	**3216.29**	**0.00**	3.17
Method	P_D=5000 RT				P_D=4000 RT				P_D=3000 RT			
	best / worst	mean	SD	average time	best / worst	mean	SD	average time	best / worst	mean	SD	average time
GA [12]	2766.31 / 3280.86	2994.23	123.97	4.96	2123.48 / 2837.19	2368.83	155.69	4.96	1533.06 / 2131.79	1751.24	153.42	5.10
PSO [12]	2587.76 / 3239.43	2706.77	163.63	**1.57**	**1922.78** / 2272.56	1984.96	97.14	**1.68**	**1363.33** / 2089.65	1498.63	147.25	**1.72**
DE [14]	2587.76 / 2650.48	2589.64	10.75	4.19	1952.11 / 2762.98	2308.12	192.71	4.02	**1363.33** / 1515.19	1377.59	20.77	4.02
IFA [15]	**2557.33** / 3578.22	2939.19	185.82	28.08	1922.79 / 2936.13	2364.70	196.63	27.97	1408.76 / 2297.29	1790.33	177.22	27.69
CNO-CL	**2557.33 / 2557.33**	**2557.33**	**0.00**	4.97	**1922.78 / 1922.78**	**1922.78**	**0.00**	4.66	**1363.33 / 1363.33**	**1363.33**	**0.00**	2.96

TABLE X
RESULTING OPERATION STATUS OF THE 20-CHILLER SYSTEM USING CNO-CL

P_D (RT)	chiller		status		PLR_i		P_i(kW)		$\sum_i^{20} P_i$(kW)
13050	#1	#2	on	on	0.99	0.91	345.43	298.07	9286.49
	#3	#4	on	on	1.00	0.76	693.80	519.99	
	#5	#6	on	on	0.99	0.91	345.43	298.07	
	#7	#8	on	on	1.00	0.76	693.80	519.99	
	#9	#10	on	on	0.99	0.91	345.43	298.07	
	#11	#12	on	on	1.00	0.76	693.80	519.99	
	#13	#14	on	on	0.99	0.91	345.43	298.07	
	#15	#16	on	on	1.00	0.76	693.80	519.99	
	#17	#18	on	on	0.99	0.91	345.43	298.07	
	#19	#20	on	on	1.00	0.76	693.80	519.99	
11600	#1	#2	on	on	0.83	0.81	238.52	231.92	7278.32
	#3	#4	on	on	0.90	0.69	566.19	419.04	
	#5	#6	on	on	0.83	0.81	238.52	231.92	
	#7	#8	on	on	0.90	0.69	566.19	419.04	
	#9	#10	on	on	0.83	0.81	238.52	231.92	
	#11	#12	on	on	0.90	0.69	566.19	419.04	
	#13	#14	on	on	0.83	0.81	238.52	231.92	
	#15	#16	on	on	0.90	0.69	566.19	419.04	
	#17	#18	on	on	0.83	0.81	238.52	231.92	
	#19	#20	on	on	0.90	0.69	566.19	419.04	
10150	#1	#2	on	on	0.73	0.74	194.50	203.94	5890.69
	#3	#4	on	on	0.72	0.65	398.28	381.42	
	#5	#6	on	on	0.73	0.74	194.50	203.94	
	#7	#8	on	on	0.72	0.65	398.28	381.42	
	#9	#10	on	on	0.73	0.74	194.50	203.94	
	#11	#12	on	on	0.72	0.65	398.28	381.42	
	#13	#14	on	on	0.73	0.74	194.50	203.94	
	#15	#16	on	on	0.72	0.65	398.28	381.42	
	#17	#18	on	on	0.73	0.74	194.50	203.94	
	#19	#20	on	on	0.72	0.65	398.28	381.42	
8700	#1	#2	on	off	0.66	0.00	173.92	0.00	4942.64
	#3	#4	on	on	0.63	0.63	334.91	365.47	
	#5	#6	on	on	0.66	0.70	173.92	190.38	
	#7	#8	on	on	0.63	0.63	334.91	365.47	
	#9	#10	on	on	0.66	0.70	173.92	190.38	
	#11	#12	on	on	0.63	0.63	334.91	365.47	
	#13	#14	on	on	0.66	0.70	173.92	190.38	
	#15	#16	on	on	0.63	0.63	334.91	365.47	
	#17	#18	on	off	0.66	0.00	173.92	0.00	
	#19	#20	on	on	0.63	0.63	334.91	365.47	
7250	#1	#2	off	off	0.00	0.00	0.00	0.00	4074.55
	#3	#4	on	on	0.64	0.63	341.82	367.28	
	#5	#6	on	off	0.67	0.00	176.36	0.00	
	#7	#8	on	on	0.64	0.63	341.82	367.28	
	#9	#10	off	off	0.00	0.00	0.00	0.00	
	#11	#12	on	on	0.64	0.63	341.82	367.28	
	#13	#14	on	off	0.67	0.00	176.36	0.00	
	#15	#16	on	on	0.64	0.63	341.82	367.28	
	#17	#18	on	off	0.67	0.00	176.36	0.00	
	#19	#20	on	on	0.64	0.63	341.82	367.28	
5800	#1	#2	off	off	0.00	0.00	0.00	0.00	3225.91
	#3	#4	on	on	0.61	0.62	325.22	362.89	
	#5	#6	off	off	0.00	0.00	0.00	0.00	
	#7	#8	on	off	0.61	0.00	325.22	0.00	
	#9	#10	on	off	0.65	0.00	170.38	0.00	
	#11	#12	on	off	0.61	0.00	325.22	0.00	
	#13	#14	on	off	0.65	0.00	170.38	0.00	
	#15	#16	on	on	0.61	0.62	325.22	362.89	
	#17	#18	on	off	0.65	0.00	170.38	0.00	
	#19	#20	on	on	0.61	0.62	325.22	362.89	

[27] J. Wang, J. Wang, and H. Che, "Task assignment for multivehicle systems based on collaborative neurodynamic optimization," *IEEE Transactions on Neural Networks and Learning Systems*, vol. 31, no. 4, pp. 1145–1154, 2020.

[28] M.-F. Leung and J. Wang, "Minimax and biobjective portfolio selection based on collaborative neurodynamic optimization," *IEEE Transactions on Neural Networks and Learning Systems*, vol. 32, no. 7, pp. 2825–2836, Jul. 2021.

[29] J. Wang, J. Wang, and Q. Han, "Multi-vehicle task assignment based on collaborative neurodynamic optimization with discrete Hopfield networks," *IEEE Transactions on Neural Networks and Learning Systems*, vol. 32, no. 12, pp. 5274–5286, Dec. 2021.

[30] M. Clerc and J. Kennedy, "The particle swarm-explosion, stability, and convergence in a multidimensional complex space," *IEEE Trans. Evol. Comput.*, vol. 6, no. 1, pp. 58–73, 2002.

[31] Y. Cao, H. Zhang, W. Li, M. Zhou, Y. Zhang, and W. A. Chaovalitwongse, "Comprehensive learning particle swarm optimization algorithm with local search for multimodal functions," *IEEE Trans. Evol. Comput.*, vol. 23, no. 4, pp. 718–731, 2019.

[32] J. Tang, G. Liu, and Q. Pan, "A review on representative swarm intelligence algorithms for solving optimization problems: Applications and trends," *IEEE/CAA J. Autom. Sin.*, vol. 8, no. 10, pp. 1627–1643, 2021.

[33] M. Hydeman, N. Webb, P. Sreedharan, and S. Blanc, "Development and testing of a reformulated regression-based electric chiller model," *ASHRAE Trans.*, vol. 108, no. 2, pp. 1118–1127, 2002.

[34] Y.-C. Chang, T.-S. Chan, and W.-S. Lee, "Economic dispatch of chiller plant by gradient method for saving energy," *Appl. Energy*, vol. 87, no. 4, pp. 1096–1101, 2010.

[35] C.-C. Lo, S.-H. Tsai, and B.-S. Lin, "Economic dispatch of chiller plant by improved ripple bee swarm optimization algorithm for saving energy," *Appl. Therm. Eng.*, vol. 100, no. 4, pp. 1140–1148, 2016.

[36] Z. Chen, J. Wang, and Q.-L. Han, "Event-triggered cardinality-constrained cooling and electrical load dispatch based on collaborative neurodynamic optimization," *IEEE Transactions on Neural Networks and Learning Systems*, pp. 1–12, 2022, in press, doi:10.1109/TNNLS.2022.3160645.

[37] P. Zhang, S. Shu, and M. Zhou, "An online fault detection method based on SVM-grid for cloud computing systems," *IEEE/CAA J. Autom. Sin.*, vol. 5, no. 2, pp. 445–456, 2018.

[38] S. Gao, M. Zhou, Y. Wang, J. Cheng, H. Yachi, and J. Wang, "Dendritic neuron model with effective learning algorithms for classification, approximation, and prediction," *IEEE Trans. Neural Netw. Learn. Syst.*, vol. 30, no. 2, pp. 601–614, 2019.

[39] Y. Sun, S. Wang, and F. Xiao, "Development and validation of a simplified online cooling load prediction strategy for a super high-rise building in Hong Kong," *Energy Convers. Manag.*, vol. 68, pp. 20–27, 2013.

[40] O. L. Mangasarian, "Pseudo-convex functions," *SIAM J Control Optim.*, vol. 3, no. 2, pp. 281–290, 1965.

This article has been accepted for publication in a future issue of this journal, but has not been fully edited. Content may change prior to final publication. Citation information: DOI 10.1109/TII.2022.3180080, IEEE Transactions on Industrial Informatics

TABLE XI
STATISTICS OF RESULTING POWER CONSUMPTION (KW) AND COMPUTATION TIME (SECONDS) FOR THE 20-CHILLER SYSTEM USING CNO-CL AND THE BASELINES

Method	P_D=13050 RT				P_D=11600 RT				P_D=10150 RT			
	best / worst	mean	SD	average time	best / worst	mean	SD	average time	best / worst	mean	SD	average time
GA [12]	9293.78 / 9401.31	9326.04	19.29	7.50	7293.64 / 7361.76	7322.59	15.50	7.51	5910.94 / 6024.68	5947.46	22.22	7.40
PSO [12]	9307.41 / 10650.73	9734.65	351.31	4.68	7942.34 / 10992.43	9149.29	658.79	4.76	6269.72 / 7563.12	6799.53	220.73	4.74
DE [14]	10188.39 / 11267.59	10746.82	219.46	7.09	7917.54 / 9502.17	8921.39	307.28	7.11	6956.12 / 8048.28	7458.87	306.82	7.05
IFA [15]	9286.71 / 9287.49	9286.98	0.17	134.02	7278.37 / 7278.58	7278.45	0.04	129.78	5890.74 / 5965.45	5896.54	19.51	129.47
CNO-CL	**9286.49 / 9286.49**	**9286.49**	**0.00**	**0.25**	**7278.32 / 7278.32**	**7278.32**	**0.00**	**4.31**	**5890.69 / 5890.69**	**5890.69**	**0.00**	**4.36**
Method	P_D=8700 RT				P_D=7250 RT				P_D=5800 RT			
	best / worst	mean	SD	average time	best / worst	mean	SD	average time	best / worst	mean	SD	average time
GA [12]	4975.30 / 5079.74	5019.05	23.24	7.39	4157.11 / 4481.54	4258.88	58.81	7.69	3322.83 / 3563.15	3437.40	57.32	7.65
PSO [12]	5080.86 / 5697.55	5407.83	126.59	**4.87**	4125.79 / 4699.08	4348.79	117.64	**4.79**	3245.64 / 3705.91	3508.28	105.54	**4.78**
DE [14]	5679.43 / 6747.46	6285.46	256.47	7.03	4423.34 / 5773.08	5164.85	272.14	7.02	3634.22 / 4624.62	4015.83	189.90	7.00
IFA [15]	4942.76 / 5005.12	4970.55	17.55	129.04	4103.48 / 4327.59	4181.83	51.55	130.60	3267.88 / 3503.05	3351.42	48.33	130.11
CNO-CL	**4942.64 / 4942.64**	**4942.64**	**0.00**	21.46	**4074.55 / 4080.84**	**4076.00**	**2.66**	62.02	**3225.91 / 3233.19**	**3226.63**	**2.20**	52.56

Zhongying Chen received the B.E. degree in building environmental and energy application engineering from Xi'an Jiaotong University, Shaanxi, China, in 2017, and the M.Sc. degree in mechanical engineering from the Hong Kong University of Science and Technology, Hong Kong, in 2018. He is a Ph.D. candidate in the Department of Computer Science, City University of Hong Kong, Hong Kong. His current research interests include optimization, computational intelligence, and energy systems.

Jun Wang (S'89–M'90–SM'93–F'07–LF'22) received his B.S. degree in electrical engineering and his M.S. degree in systems engineering from Dalian University of Technology, Dalian, China, in 1982 and 1985, respectively, and his Ph.D. degree in systems engineering from Case Western Reserve University Cleveland, Ohio, USA, in 1991.

He held various academic positions at Dalian University of Technology, Dalian, China; Case Western Reserve University, Cleveland, OH, USA; University of North Dakota, Grand Forks, ND, USA; and the Chinese University of Hong Kong. He also held various short-term or part-time visiting positions at the USAF Armstrong Laboratory, Dayton, OH, USA; RIKEN Brain Science Institute, Tokyo, Japan; Huazhong University of Science and Technology, Wuhan, China; Shanghai Jiao Tong University, Shanghai, China; and Dalian University of Technology, Dalian, China. He is currently a chair professor in the Department of Computer Science and School of Data Science at City University of Hong Kong, Kowloon, Hong Kong.

He was the Editor-in-Chief of the *IEEE TRANSACTIONS ON CYBERNETICS* in 2014-2019. He also served on the Editorial Board or Editorial Advisory Board of the IEEE TRANSACTIONS ON NEURAL NETWORKS, IEEE TRANSACTIONS ON SYSTEMS, MAN, AND CYBERNETICS-PART C, *Neural Networks*, and *International Journal of Neural Systems*. He was a Guest Editor of special issues of several journals such as the *European Journal of Operational Research*, and *International Journal of Neural Systems*. He served as the General Chair of the IEEE World Congress on Computational Intelligence in 2008, 13th/25th International Conference on Neural Information Processing in 2006/2018.

He is a Fellow of the International Association for Pattern Recognition and a foreign member of Academia Europaea. He was a recipient of the Research Excellence Award from The Chinese University of Hong Kong for 2008-2009, the Outstanding Achievement Award from Asia Pacific Neural Network Assembly, *IEEE TRANSACTIONS ON NEURAL NETWORKS* Outstanding Paper Award in 2011, Neural Networks Pioneer Award from the IEEE Computational Intelligence Society in 2014, Norbert Wiener Award from the IEEE Systems, Man and Cybernetics Society in 2019, among other distinctions.

Qing-Long Han (Fellow, IEEE) received the B.Sc. degree in Mathematics from Shandong Normal University, Jinan, China, in 1983, and the M.Sc. and Ph.D. degrees in Control Engineering from East China University of Science and Technology, Shanghai, China, in 1992 and 1997, respectively.

Professor Han is Pro Vice-Chancellor (Research Quality) and a Distinguished Professor at Swinburne University of Technology, Melbourne, Australia. He held various academic and management positions at Griffith University and Central Queensland University, Australia. His research interests include networked control systems, multi-agent systems, time-delay systems, smart grids, unmanned surface vehicles, and neural networks.

Professor Han was awarded The 2021 Norbert Wiener Award (the Highest Award in systems science and engineering, and cybernetics) and The 2021 M. A. Sargent Medal (the Highest Award of the Electrical College Board of Engineers Australia). He was the recipient of The 2021 IEEE/CAA Journal of Automatica Sinica Norbert Wiener Review Award, The 2020 IEEE Systems, Man, and Cybernetics (SMC) Society Andrew P. Sage Best Transactions Paper Award, The 2020 IEEE Transactions on Industrial Informatics Outstanding Paper Award, and The 2019 IEEE SMC Society Andrew P. Sage Best Transactions Paper Award.

Professor Han is a Member of the Academia Europaea (The Academy of Europe) and a Fellow of The Institution of Engineers Australia. He is a Highly Cited Researcher in both Engineering and Computer Science (Clarivate Analytics). He has served as an AdCom Member of IEEE Industrial Electronics Society (IES), a Member of IEEE IES Fellows Committee, and Chair of IEEE IES Technical Committee on Networked Control Systems. He is Co-Editor-in-Chief of IEEE Transactions on Industrial Informatics, Deputy Editor-in-Chief of IEEE/CAA JOURNAL OF AUTOMATICA SINICA, Co-Editor of Australian Journal of Electrical and Electronic Engineering, an Associate Editor for 12 international journals, including the IEEE TRANSACTIONS ON CYBERNETICS, IEEE INDUSTRIAL ELECTRONICS MAGAZINE, Control Engineering Practice, and Information Sciences, and a Guest Editor for 14 Special Issues.